Catalytically Distinct Antibodies Prepared by the Reactive Immunization versus Transition State Analogue Hapten Manifolds

Anita Datta, Paul Wentworth, Jr.,* Joanne P. Shaw, Anton Simeonov, and Kim D. Janda*

Contribution from the Department of Chemistry, The Scripps Research Institute and the Skaggs Institute for Chemical Biology, 10550 North Torrey Pines Road, La Jolla, California 92037

Received April 20, 1999

Abstract: This report describes the first direct comparison between the reactive immunization and transition state analogue hapten manifolds for catalytic antibody production. In an initial communication (Janda et al *J. Am. Chem. Soc.* **1997**, *119*, 10251) we described the use of a phosphonate diester hapten **5**, in a reactive immunization approach, that elicited a panel of proficient biocatalysts for the hydrolysis of *S*-(+)-naproxen *p*-methylsulfonylphenyl ester (**3b**) [k_{cat}(**3b**)/k_{uncat}(**3b**) = 0.05−6.60 × 10^5]. However, only moderate enantioselectivity was obtained when the panel of antibody catalysts was studied in a kinetic resolution of *rac*-**3a**, the best result leading to *S*-(+)-**4a** in 90% ee for 35% conversion of *rac*-**3a**. This report details a transition state analogue hapten approach to elicit antibody catalysts for this same process by employment of phosphonate monoester **6**. This strategy has yielded a library of catalysts with excellent turnover numbers [k_{cat}(**3b**)/k_{uncat}(**3b**) = 0.14−19.0 × 10^5] and enantioselectivities. Three of these catalysts, 6G6, 12C8, and 12D9, perform a useful kinetic resolution of *rac*-**3a**, generating *S*-(+)-naproxen **4a** in >98% ee with up to 50% conversion. Comparing the two hapten strategies reveals that the antibodies, although elicited for the same reaction with the same substrate, exhibit quite different catalytic behavior. The transition state analogue approach has furnished better catalysts, in terms of turnover numbers and enantiomeric discrimination, but which possess varying degrees of product inhibition by phenol **9**. Thermodynamic evaluation reveals that their catalytic power is derived almost entirely as a function of differential stabilization of the transition state over the ground state: K_m(**3b**)/K_i(**8**). By contrast, the reactive immunization approach has elicited more proficient biocatalysts that couple an efficient "catalytic" mechanism and improved substrate recognition with no product inhibition.

Introduction

The catalysis of acyl-transfer processes is ubiquitous in both biochemical metabolism and organic chemistry and as such has remained a major target for catalytic antibodies since the first reports of these tailor-made proteins emerged.[1,2] Most reactions of this type involve the stepwise addition of a nucleophile followed by expulsion of the leaving group with a transient, high-energy, tetrahedral intermediate (TI^-) separating these processes. The guiding methodology to elicit antibody catalysts for these reactions has been the use of stable transition state analogues as haptens and the scope and limitations of this approach is an ongoing area of study.[3,4] In addition, new hapten strategies, such as bait-and-switch[5−7] and heterologous immunization,[8,9] are being developed to push back the boundaries of the catalytic abilities and scope of the antibodies thus generated. However, only by directly comparing these new methods with the standard transition state analogue approach can a full appreciation of both their benefits and drawbacks be realized.

Reactive immunization,[10] the most recent hapten manifold to be exploited by the catalytic antibody field, has thus far led to the production of biocatalysts for both aryl ester hydrolyses[10,11] and aldol condensation reactions with broad substrate tolerance.[12] The key to this strategy, as the name implies, is immunization with a hapten that can "react" with antibody binding-site residues at the B-cell level of the immune response. These residues then partake in a "catalytic" mechanism when the antigen is switched for the substrate. Two classes of haptens have been thus far explored: phosphonate diesters **1** and β-diketones **2** (Figure 1).

The classical view of how the immune system responds to a given antigen is centered around the premise of increasing affinity and selectivity of antibody−antigen binding. At the molecular level this process involves the utility of a primary immune repertoire of ≈10^8 antibody members enhanced by

* To whom correspondence should be addressed.

(1) Tramontano, A.; Janda, K. D.; Lerner, R. A. *Proc. Natl. Acad. Sci. U.S.A.* **1986**, *83*, 6736−6740.
(2) Pollack, S. J.; Jacobs, J. W.; Schultz, P. G. *Science* **1986**, *234*, 1570−1573.
(3) Wentworth, P., Jr.; Janda, K. D. *Curr. Opin. Chem. Biol.* **1998**, *2*, 138−144.
(4) Blackburn, G. M.; Datta, A.; Denham, H.; Wentworth, P., Jr. *Adv. Phys. Org. Chem.* **1998**, *31*, 249−392.
(5) Janda, K. D.; Weinhouse, M. I.; Schloeder, D. M.; Lerner, R. A.; Benkovic, S. J. *J. Am. Chem. Soc.* **1990**, *112*, 1274−1275.
(6) Janda, K. D. *Biotechnol. Prog.* **1990**, *6*, 178−181.
(7) Janda, K. D.; Weinhouse, M. I.; Danon, T.; Pacelli, K. A.; Schloeder, D. M. *J. Am. Chem. Soc.* **1991**, *113*, 5427−5434.
(8) Suga, H.; Ersoy, O.; Williams, S. F.; Tsumuraya, T.; Margolies, M. N.; Sinskey, A. J.; Masamune, S. *J. Am. Chem. Soc.* **1994**, *116*, 6025−6026.
(9) Tsumuraya, T.; Suga, H.; Meguro, S.; Tsunakawa, A.; Masamune, S. *J. Am. Chem. Soc.* **1995**, *117*, 11390−11396.
(10) Wirsching, P.; Ashley, J. A.; Lo, C.-H. L.; Janda, K. D.; Lerner, R. A. *Science* **1995**, *270*, 1775−1782.
(11) Lo, C.-H. L.; Wentworth, P., Jr.; Jung, K. W.; Yoon, J.; Ashley, J. A.; Janda, K. D. *J. Am. Chem. Soc.* **1997**, *119*, 10251−10252.
(12) Wagner, J.; Lerner, R. A.; Barbas, C. F., III *Science* **1995**, *270*, 1797−1800.

10.1021/ja991274t CCC: $18.00
Published on Web 10/23/1999

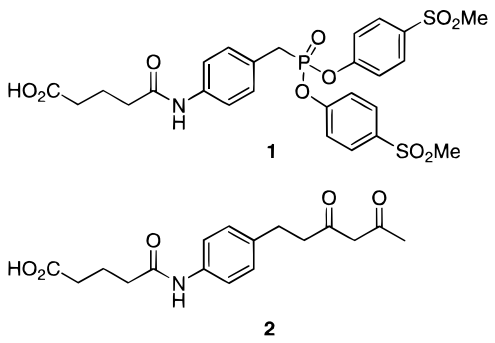

Figure 1. The two classes of haptens utilized for reactive immunization: phosphonate diesters **1** and β-diketones **2**.

somatic mutations and recombinations within the antibody gene set so as to generate a library of focused functional proteins that optimize spatial and electrostatic noncovalent interactions with the antigen. However, in a reactive immunization this classical notion is challenged. It has been suggested that following the "reaction" between an antibody binding-site residue and the reactive immunogen further evolution of the immune response to the antigen is arrested.[13] The principle of antibody maturation, a process driven by a competition for binding energy, lends support to this theory as no stronger interaction can be made between an antibody and its antigen than a covalent linkage. This suggests that the fine-tuning of antibody−antigen complementarity is linked to the point within the evolution of the immune response at which the "reactive" immunogen is trapped by the antibody binding-site residue. This could have implications for the catalytic antibody field in terms of both the substrate specificity and the kinetic proficiency of any biocatalysts elicited by this approach.

Recently we communicated that a reactive immunization hapten **5** elicited a library of antibody catalysts for the kinetic resolution of naproxen *p*-methylsulfonylphenyl esters (*rac*-**3a**) but that the observed ee values of *S*-(+)-naproxen (**4a**) were too low to be of commercial utility (Scheme 1).[11] Chemical synthesis of *S*-(+)-**4a** involves diastereomeric crystallization from a racemic acid mixture.[14] Therefore there is considerable effort being directed toward improving the methods for both its asymmetric synthesis and resolution.[15−18] Herein we report the characterization of an additional library of antibodies, generated in this case against the corresponding transition state analogue hapten **6**, which catalyze the same enantioselective hydrolysis of *rac*-**3a**. Both sets of biocatalysts have been analyzed in terms of their kinetic efficiencies, thermodynamic binding properties, mechanisms, and enantioselectivities to help elucidate how these two hapten strategies differ in terms of the catalysts they generate.

Results and Discussion

Hapten Design and Synthesis and Antibody Production. Much of the initial work in the catalytic antibody field has focused on the acceleration of facile reactions that proceed through a single high-energy intermediate that differs considerably from the ground state, for example ester hydrolysis. Many haptenic structures have proved successful in the generation of efficient catalysts ($k_{cat}/k_{uncat} > 10^4$) and their relative merits have been extensively reviewed.[3,4,19] The transition state analogue hapten **6** used in this comparative study was designed essentially by precedent.

In the original reactive immunization approach no stereocontrol was employed during the synthesis of hapten **5** and therefore the methyl group at the key locus, α to the phosphonate diester center, is stereochemically undefined.[11] By immunizing with a racemic hapten it was hoped to exploit the known enantiomeric discrimination inherent within the immune system to generate enantioselective catalysts.[20,21] Consequently, to allow a more direct comparison with the reactive immunization approach, the phosphonate monoester hapten **6** was also immunized as a racemic mixture.

The phosphonate diester hapten **5** and methoxy ether inhibitors **7** and **8** were synthesized as described previously.[11] The transition state analogue hapten **6** was synthesized in 98% yield by hydrolysis of the phosphonate diester **5** with lithium hydroxide. Phosphonate monoester **6** was coupled to the carrier proteins bovine serum albumin (BSA) and keyhole limpet hemocyanin (KLH) by prior activation with sulfo-*N*-hydroxysuccinimide and EDC. The KLH-**6** conjugate was used to immunize 129GIx mice. Following antibody production by standard hybridoma technology,[22,23] 28 monoclonal antibodies were generated that bound to a BSA-**6** conjugate. All the monoclonal antibodies were of the IgG class and were purified as described previously.[11] Antibodies were judged to be homogeneous by sodium dodecyl sulfate (SDS)-polyacrylamide gel electrophoresis.

Kinetic Evaluation. From the 28 monoclonal antibodies that were elicited to hapten **6**, 12 were found to catalyze the hydrolysis of *rac*-**3a**. By comparison, 12 of 20 clones elicited to the reactive immunization hapten **5** possessed analogous catalytic activity.[11] The five most active catalysts within each library were characterized in detail and the results are presented in Table 1.

All 10 antibodies catalyze the hydrolysis of **3a**−**c** in accordance with the Michaelis−Menten model and perform multiple turnovers without a detectable loss in activity. The most efficient antibody, 6G6, has a turnover number [k_{cat}(**3b**)] of 81 min^{-1} that is equivalent to a $k_{cat}(\mathbf{3b})/k_{uncat}(\mathbf{3b})$ of 1.19×10^6. Comparison of the enhancement ratios, $k_{cat}(\mathbf{3b})/k_{uncat}(\mathbf{3b})$, for each antibody reveals that the transition state analogue approach has furnished, on the whole, the most active catalysts. However, a more meaningful method of comparing biocatalysts is to assess their performance at substrate concentrations below K_m, as represented by the apparent-second-order specificity constant k_{cat}/K_m.[24] Such an analysis highlights that it is the reactive immunization antibodies that, in general, are the most proficient catalysts even approaching enzyme-like activity: 5A9 $k_{cat}(\mathbf{3b})/K_m(\mathbf{3b}) = 2.0 \times 10^5\ M^{-1}\ s^{-1}$ (Table 1).

The catalytic activity of the transition state analogue antibodies is competitively inhibited by hapten analogue **8**. Preliminary studies revealed that the inhibition constants, K_i(**8**), would be

(13) Barbas, C. F., III; Hiene, A.; Zhong, G.; Hoffmann, T.; Gramatikova, S.; Björnestedt, R.; Liszt, B.; Anderson, J.; Stura, E. A.; Wilson, I. A.; Lerner, R. A. *Science* **1997**, *278*, 2085−2092.
(14) Harrison, I. T.; Lewis, B.; Nelson, P.; Rooks, W. H. I.; Roszowski, A. P.; Tomolonis, A.; Fried, J. H. *J. Med. Chem.* **1970**, *13*, 203−207.
(15) Gu, Q.-M.; Chen; C.-S.; Sih, C. J. *Tetrahedron Lett.* **1986**, *27*, 1763−1766.
(16) Hernaiz, M. J.; Sanchez-Montero, J. M.; Sinisterra, J. V. *Tetrahedron* **1994**, *50*, 10749−10760.
(17) Manimaran, T.; Stahly, G. P. *Tetrahedron Asymmetry* **1993**, *4*, 1949−1954.
(18) Pirkle, W. H.; Liu, Y. *J. Org. Chem.* **1994**, *59*, 6911−6916.
(19) MacBeath, G.; Hilvert, D. *Chem. Biol.* **1996**, *3*, 433−445.
(20) Janda, K. D.; Benkovic, S. J.; Lerner, R. A. *Science* **1989**, *244*, 437−440.
(21) Fujii, I.; Lerner, R. A.; Janda, K. D. *J. Am. Chem. Soc.* **1991**, *113*, 8528−8529.
(22) Köhler, G.; Howe, S. C.; Milstein, C. *Eur. J. Immunol.* **1976**, *6*, 292−295.
(23) Köhler, G.; Milstein, C. *Nature* **1975**, *256*, 495−497.
(24) Fersht, A. R. *Proc. R. Soc. London B* **1974**, *187*, 397−407.

Scheme 1. Substrates **3a-c**, Products **4a,b**, Haptens **5** and **6**, and Inhibitors **7** and **8** Utilized for a Comparison of the Reactive Immunization and Transition State Analog Hapten Manifolds for the Elicitation of Antibody Aryl Esterases

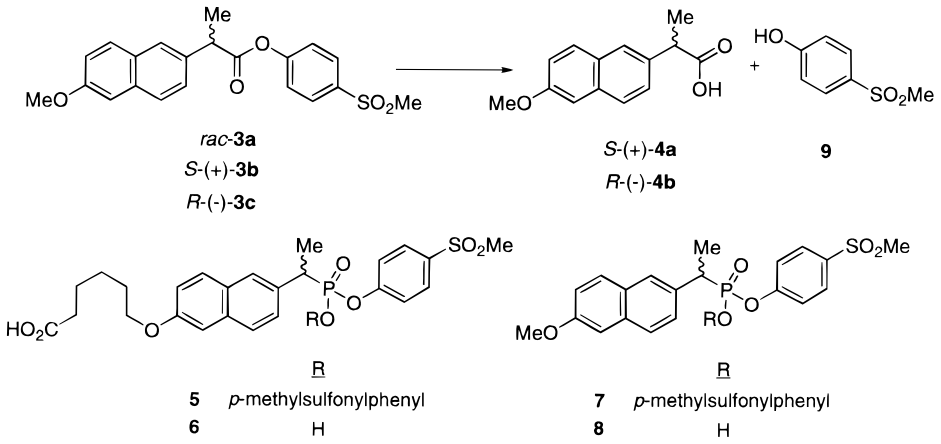

Table 1. Kinetic Parameters[a] for Antibodies Elicited by the Transition State Analog (**6**) and Reactive Immunization (**5**) Haptens

antibody	isotype[b]	k_{cat}(**3b**)/min^{-1}	ER[c]/10^5	K_m(**3b**)/μM	k_{cat}/K_m/10^4 M^{-1} s^{-1}	K_i(**8**)[d]/μM	K_i(**7**)/μM
transition state analogue library[e]							
6G6	$\kappa\gamma_1$	81 ± 3.5	19	890 ± 48	4.5	0.004 ± 0.0004	—[f]
9B1	$\kappa\gamma_1$	5.8 ± 0.38	1.4	1900 ± 230	0.3	0.043 ± 0.003	—[f]
12C8	$\kappa\gamma_1$	51 ± 3.8	12	760 ± 58	3.4	0.012 ± 0.003	—[f]
12D9	$\kappa\gamma_1$	14 ± 1.3	3.2	510 ± 35	2.7	0.011 ± 0.002	—[f]
11C10	$\kappa\gamma_1$	0.6 ± 0.02	0.14	1400 ± 170	0.04	98 ± 1.2	—[f]
reactive immunization library							
15G12	$\kappa\gamma_{2a}$	28 ± 2.5	6.6	300 ± 45	9.3	150 ± 18	0.95 ± 0.10
7H9	$\kappa\gamma_{2a}$	3.3 ± 0.48	0.78	580 ± 65	5.7	110 ± 8.7	4.0 ± 0.03
5A9	$\kappa\gamma_{2a}$	2.3 ± 0.19	0.54	10 ± 1.2	20	1.4 ± 0.11	2.0 ± 0.15
7E1	$\kappa\gamma_{2a}$	1.6 ± 0.25	0.38	210 ± 27	0.8	150 ± 8.5	3.0 ± 0.28
6C7	$\kappa\gamma_{2a}$	0.2 ± 0.02	0.05	2.0 ± 0.3	10	0.55 ± 0.028	0.15 ± 0.09

[a] Kinetic assays were performed in aqueous buffer (100 mM bicine, pH 8.0) with 4% DMF and 1% Tween 80 as cosolvents. The reaction was followed by monitoring formation of acid *S*-(+)-**4a** by reversed phase HPLC. Kinetic parameters were then determined by nonlinear regression and Lineweaver−Burke analyses of the initial rate data with the EnzymeKinetics v1.1 computer program, Trinity Software (copyright 1990−1991). [b] Isotyping was performed using a standard enzyme-linked immunosorbent assay. [c] Enhancement ratio k_{cat}(**3b**)/k_{uncat}(**3b**), k_{uncat}(**3b**) = 4.5 × 10^{-5} min^{-1}. [d] K_i determination with inhibitors **8** and **7** was performed by initial IC_{50} measurement and then transformation of these data using the method of Copeland et al.[25] For limitations associated with this analysis see ref 25. [e] Significant curving in the progress curves was noted for all the panel of antibodies, therefore initial rates were determined from the first 1−2% of the reaction. [f] Not measured.

in the nanomolar range which was comparable to the antibody concentrations being used for the assays. Under these conditions, determination of K_i values by Lineweaver−Burke analysis is invalid because the concentration of antibody-inhibitor complex formed during the assay affects the total inhibitor concentration in solution. Therefore we employed the method of Copeland et al.[25] which involves the experimental measurement of IC_{50} (inhibitor concentration which reduces the catalytic activity to 50%), followed by an estimation of the K_i value using eq 1:

$$K_i = IC_{50} - ([E_t]/2)/(1 + [S]/K_m) \quad (1)$$

where $[E_t]$ = total antibody binding-site concentration and [S] = substrate concentration. The K_i values for the transition state analogue antibodies are shown in Table 1.

Mechanistic Evaluation. The relationship between the catalytic activity of an antibody and the differential binding of the transition state relative to ground state can be most clearly visualized by the use of a thermodynamic cycle based on transition state theory. The key relationship is that $K_m/K_i \approx k_{cat}/k_{uncat}$. Such an analysis has been shown to be equally valid for enzymes with transition state analogue inhibitors[26] and catalytic antibodies with their transition state analogue immunogen.[27,28] The panel of antibodies elicited by the transition state analogue hapten **6** follow this thermodynamic equivalence over the 2 orders of magnitude in K_m(**3b**)/K_i(**8**) present within the library, laying slightly above but parallel (gradient = + 0.905, r^2 = 0.898) to the theoretical line (gradient = + 1.0) (Figure 2).

However, the evolution of optimal binding toward the transition state is reflected by poor recognition of the ground state. This is evident from the 10^6-fold difference in K_m(**3b**) and K_i(**8**) values for the transition state analogue antibodies, and it is this deficiency that reduces their relative proficiency constants, k_{cat}(**3b**)/K_m(**3b**). This observed limitation, the evolution to bind only one species along the reaction coordinate, enforces transition state stabilization as the major determinant of antibody catalysis. Enzymes by contrast, through evolutionary pressure, have developed the ability to recognize and bind dynamically to all the intermediates that link substrates and products along the reaction pathway.[29,30]

The next phase of the studies focused on investigating the catalytic mechanism of the reactive immunization antibody panel. For compounds to be considered as potential haptens for reactive immunization they have to possess sufficient reactivity to undergo a chemical reaction within the antibody binding site, but be sufficiently stable so as not to be completely decomposed

(25) Copeland, R. A.; Lombardo, D.; Giannaras, J.; Decicco, C. P. *Bioorg. Med. Chem. Lett.* **1995**, *5*, 1947−1952.
(26) Wolfenden, R. A. *Annu. Rev. Biophys. Bioeng.* **1976**, *5*, 271−306.
(27) Jacobs, J. W. *Bio./Technol.* **1991**, *9*, 258−262.
(28) Stewart, J. D.; Benkovic, S. J. *Nature* **1995**, *375*, 388−391.
(29) Albery, J.; Knowles, J. R. *Biochemistry* **1976**, *15*, 5631−5640.
(30) Albery, J.; Knowles, J. R. *Angew. Chem., Int. Ed. Engl.* **1977**, *16*, 285−293.

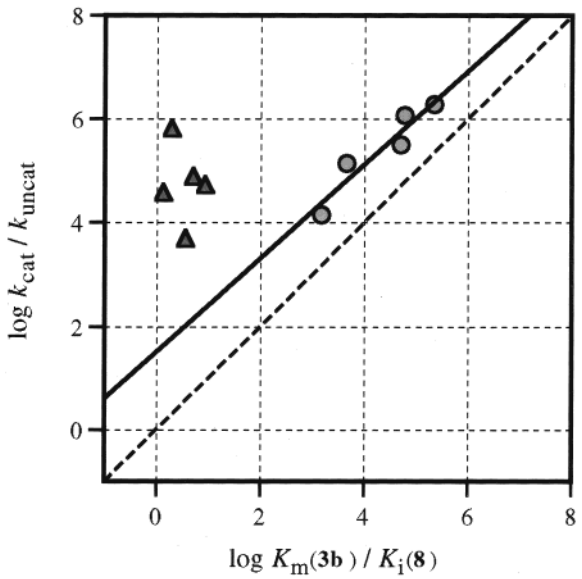

Figure 2. Comparison of the differential binding energy, K_m(**3b**)/K_i(**8**), with observed catalytic rate, k_{cat}(**3b**)/k_{uncat}(**3b**), for antibody-catalyzed hydrolysis of ester *S*-(+)-**3b**. The two data sets presented are the libraries of transition state analogue (circle) and reactive immunization antibodies (triangle). The hatched line (gradient +1) is included for reference and is not fit to the data. The solid line (gradient +0.905, $r^2 = 0.898$) is a linear correlation fitted to the transition state analogue antibody data.

Scheme 2. Spontaneous in Vivo Hydrolysis of the Phosphonate Diester Hapten **5** to the Stable Phosphonate Monoester **6**[a]

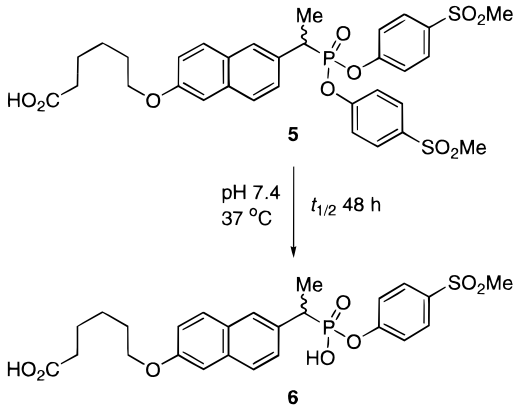

[a] The half-life of 48 h was determined in vitro (pH 7.4 at 37 °C).

before the immune system has a chance to evolve a response.[10] The half-life for decomposition of the phosphonate diester hapten **5** into **6** under conditions designed to mimic its in vivo hydrolysis [pH 7.4 (PBS 20 mM) at 37 °C] is 48 h, and consequently evolution of the immune response should be a composite of recognition toward both molecules (Scheme 2).

It was important for us to show that the panel of antibodies elicited to the reactive immunogen **5** had not, by nature of its spontaneous hydrolysis, simply been programmed by recognition of its breakdown product **6**. For this reason we performed the same thermodynamic cycle analysis, K_m(**3b**)/K_i(**8**) ≈ k_{cat}(**3b**)/k_{uncat}(**3b**), for the reactive immunization antibodies as described *vide supra* (see Figure 2). In this study hapten analogue **8** is being used, essentially as a probe, to detect if any of the reactive immunization antibodies utilize a reaction pathway for which inhibitor **8** is a transition state analogue. Figure 2 shows that, in contrast to the transition state analogue antibodies elicited to **6**, where there is a very good correlation of K_m(**3b**)/K_i(**8**) ≈ k_{cat}(**3b**)/k_{uncat}(**3b**), no correlation exists for the antibody catalysts elicited by reactive immunization with **5**. For example, antibody 5A9 has a ratio of K_m(**3b**)/K_i(**8**) of 8.6 yet this clone displays an enhancement ratio k_{cat}(**3b**)/k_{uncat}(**3b**) = 5.4×10^4. These results provide strong evidence that the catalytic power imparted by the reactive immunization antibodies is not linked simply to stabilization of a transition state mimicked by phosphonate monoester **8**, and hence that these antibodies were not elicited solely to the hydrolysis product **6** of the reactive immunogen **5**.

Table 2. Apparent Equilibrium Dissociation Constant $K_d$app Determinations[a] for the Panel of Antibodies Elicited by Reactive Immunization Hapten **5**

antibody	K_{dapp}(**8**)/μM	$K_d$app(**7**)/μM
15G12	1.3	0.42
7H9	2.1	0.44
5A9	0.9	0.52
7E1	1.8	0.6
6C7	2.4	1.0

[a] Apparent binding constant measured by a competition ELISA procedure; see Experimental Section for details.

Thus far, the actual mechanism by which the reactive immunization antibodies catalyze the efficient hydrolysis of *S*-(+)-**3b** remains unresolved. A covalent "reaction" between the antibody and the reactive immunogen to generate a nucleophilic binding-site residue during the immune response has been postulated as the *modus operandi* of this approach.[10] A number of observations have been made which support the utility of a residue acting in either a covalent manner or as a general base. For example, the reactive immunization antibodies do react with hapten analogue **7**; the kinetics of this process were determined for antibody 15G12 which catalyzes the hydrolysis of hapten analogue **7** to **8** with release of phenol **9** [K_m(**7**) = 232 μM, k_{cat}(**7**) = 2.1×10^{-3} min^{-1}].[11] The putative phosphonylated-15G12 intermediate was sufficiently labile that dephosphonylation was not rate determining and thus no accumulation of the antibody-phosphonyl intermediate occurred. This observation was also noted in the seminal reactive immunization paper.[10] However, attempts to link a "covalent" mechanism to the hydrolysis of the substrate ester *S*-(+)-**3b** have thus far proved unfruitful. No evidence for the accumulation of an acyl-antibody intermediate during the hydrolysis of *S*-(+)-**3b** has yet been obtained. This of course does not preclude its existence, but implies that deacylation of any such acyl-antibody complex cannot be rate limiting under the assay conditions.[31]

Substrate Binding. The reactive immunization antibody panels have, on the whole, lower K_m(**3b**) values (2 to 576 μM) relative to the transition state analogue antibodies (513 to 1950 μM). As described *vide supra*, catalytic antibody hydrolases elicited to transition state analogues are relatively simple biocatalysts having evolved primary recognition of only the TI$^-$ along the reaction coordinate thus explaining their poor substrate binding properties.

The *in vivo* hyperimmunization process takes approximately 6 months, and therefore, the immune system is exposed to the reactive immunogen **5** ($t_{1/2}$ = 48 h) for only a small fraction of that time. Apparent equilibrium binding constants $K_d$app, measured by competition ELISAs, highlight the fact that the reactive immunization antibody panels possess slightly higher affinity for the reactive immunization hapten analogue **7** (0.42 to 1.0 μM) than for the transition state analogue hapten analogue **8** (0.9 to 2.4 μM) (Table 2).

(31) Lolis, E.; Petsko, G. A. *Annu. Rev. Biochem.* **1990**, *59*, 597−630.

Table 3. Product Inhibition Data by Phenol **9** with the Transition State Analog **6** Derived Antibody Library

antibody	activity[a] with **9**, %	activity with **4a,** %
6G6	28 [K_i[b](**9**) = 50 μM]	98
12C8	56	96
9B1	95	100
12D9	34	94
11C10	40	99

[a] Activity is defined as the ratio of the absolute rates of the antibody-catalyzed hydrolysis of ester *S*-(+)-**3b** (200 μM) with and without phenol **9** (50 μM) or acid *S*-(+)-**4a** (50 μM) as a percentage. [b] K_i(**9**) (measured at pH 8.0) was determined by the method described *vide supra* (see ref 25).

Furthermore, a comparison between the $K_d$app(**7**) with the K_m(**3b**) for each of the reactive immunization antibodies (see Tables 1 and 2) reveals that the differential binding of hapten and substrate varies from a factor of only 2 for antibody 6C7, to 1.3×10^3 for antibody 7H9. This hapten−substrate affinity difference is considerably lower than that observed for the transition state analogue antibodies *vide supra*. These data suggest that, during the reactive immunization with **5**, there has been a lack of maturation of the immune response to the immunogen. This has led to the elicitation of a panel of antibodies with relatively nonspecific combining sites that can bind, with similar affinity, to molecules that share common structural features with the reactive immunogen **5**. It is this arrested evolution of the reactive immunization antibodies toward the immunogen **5** that allows the antibodies to exhibit relatively good substrate recognition properties.

Whether this lack of maturation of the immune response during a reactive immunization is a general phenomenon is still unclear. However, Lerner[13] has recently suggested that the broad substrate tolerance exhibited by a catalytic antibody elicited to a β-diketone reactive immunogen is a direct result of a poorly evolved immune response during the immunization process.

Product Binding. As critical to a successful biocatalytic process as the ability to efficiently bind and transform substrate, is the facility to release products. Antibodies elicited by the transition state analogue approach are known to suffer from product inhibition, though this is by no means a universal problem.[3,4,19] During the kinetic studies with the transition state analogue antibodies and substrate *S*-(+)-**3b** significant curving in the progression curves was observed. Therefore each product, phenol **9** and carboxylate *S*-(+)-**4a**, was tested for its ability to inhibit the activity of the transition state analogue antibodies. For all the antibodies in the panel, the catalysis was inhibited by *p*-methylsulfonyl phenol **9** but not by *S*-(+)-naproxen **4a** (Table 3). The inhibition of antibody 6G6 by phenol **9** was the most significant and was studied in some detail. The inhibition was found to be competitive in nature, with a K_i(**9**) = 50 μM. Interestingly, the inhibitory effect of **9** was neither reduced nor enhanced by performing the 6G6 assay at pH 6.5, where the phenol is >95% protonated (pK_a of **9** = 7.8), instead of the standard assay conditions at pH 8.0. This suggests that antibody recognition of **9** is not perturbed by its phenolate/phenol equilibrium.

The inhibition by phenol **9** is rationalized as being a result of the location of the linker in hapten **6**. Antibody-hapten recognition is optimal at loci opposite to the point of linker attachment.[32] Therefore phenol **9** may well be buried deep within the antibody binding site, whereas the carboxylate **4a** should be more solvent exposed.

By contrast none of the reactive immunization antibodies elicited in this study suffer from inhibition by either phenol **9** or carboxylate **4a**. This was quite surprising considering the fact that the reactive immunization antibodies seem to possess binding properties to molecules sharing structural similarities to immunogen **5**, *vide supra*. Furthermore, in the seminal report of the reactive immunization hapten strategy significant product inhibition was observed.[10] However, this study shows that product inhibition is not necessarily a trademark of reactive immunization strategy when using phosphonate diesters as haptens.

Antibody Enantioselectivity. The antibodies elicited by reactive immunization possess excellent enantiomeric discrimination, as determined from their respective *E* values[33] (20−123):[11] the ratio of the pseudo-second-order specificity constants for the antibody-catalyzed hydrolysis of the enantiomeric esters *S*-(+)-**3b** or *R*-(−)-**3c**. However, the antibody-catalyzed kinetic resolutions of *rac*-**3a** give only low to moderate ee values of *S*-(+)-**4a**. The most efficient clone is antibody 5A9, which gives *S*-(+)-**4a** in 90% ee for 35% conversion of *rac*-**3a**. The source of this anomaly, high *E* value versus low ee, was found to be a result of competitive inhibition by the slow reacting enantiomer, *R*-(−)-**3c**. The positive effects of broad recognition *vide supra* manifest themselves here in a negative fashion by not supplying sufficient enantiomeric discrimination to perform a successful kinetic resolution.

All the transition state analogue antibodies in Table 1 are enantioselective catalysts, each catalyzing the hydrolysis of *S*-(+)-**3b** more efficiently than *R*-(−)-**3c**. However, accurate determination of the kinetic parameters of the antibodies with ester *R*-(−)-**3c**, and hence the *E* values, has not been possible because it is such a poor substrate. Antibody-catalyzed hydrolysis of *R*-(−)-**3c** is typically 2−3 orders of magnitude lower than that observed with *S*-(+)-**3b**. In addition, the K_m(**3c**) is also much higher than that for *S*-(+)-**3b**, such that in the accessible substrate range (up to 900 μM) no saturation in the antibody-catalyzed rate is observed. However, as expected from the poor binding and turnover of *R*-(−)-**3c**, the transition state analogue antibodies do catalyze the kinetic resolution of *rac*-**3a**. By comparison with the reactive immunization antibodies, rate studies reveal that the transition state antibody-catalyzed rates of hydrolysis of *rac*-**3a** are not inhibited by *R*-(−)-**3c** (data not shown). Three antibodies from the transition state analogue panel, 12C8, 12D9, and 6G6, have been studied in detail and all give >98% ee of *S*-(+)-**4a** for up to 50% conversion of *rac*-**3a**. The time course of the kinetic resolution of *rac*-**3a** catalyzed by antibody 12C8 is shown in Figure 3. The transition state analogue approach has clearly yielded more "useful" biocatalysts than the reactive immunization approach for this kinetic resolution.

Conclusion

Jencks' seminal postulate that eliciting antibodies to stable transition state analogues could lead to the generation of a new class of biocatalysts is now standard dogma.[34] The vast body of evidence already accrued suggests that this guiding methodology can yield k_{cat}/k_{uncat} values of up to 10^7, equivalent to a differential binding energy $K_m/K_i \approx 10$ kcal mol^{-1}.[4,28] Reactive immunization, which incorporates chemical reactivity coupled with broader substrate tolerance, offers the potential to generate

(32) Wentworth, P., Jr.; Datta, A.; Smith, S.; Marshall, A.; Partridge, L. J.; Blackburn, G. M. *J. Am. Chem. Soc.* **1997**, *119*, 2315−2316.

(33) Chen, C.-S.; Wu, S.-H.; Girdaukas, G.; Sih, C. J. *J. Am. Chem. Soc.* **1987**, *109*, 2812−2817.

(34) Jencks, W. P. *Mechanisms for Catalysis*; McGraw-Hill: New York, 1969; pp 3−6.

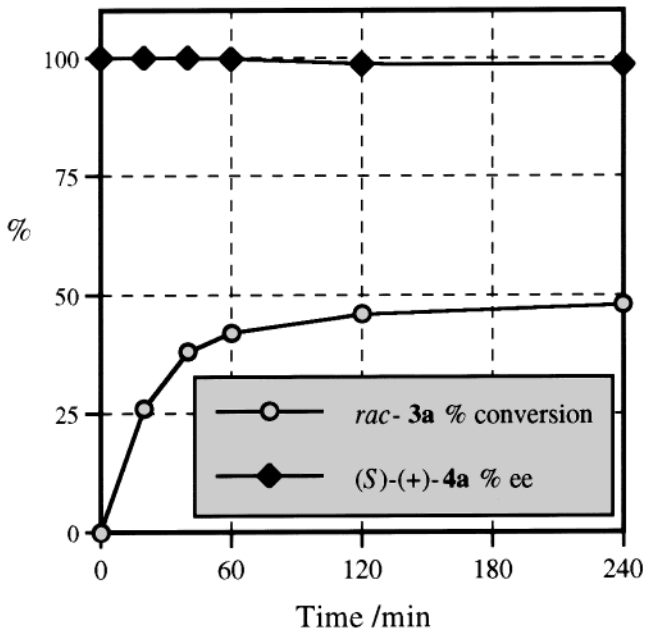

Figure 3. Antibody, 12C8, catalyzed kinetic resolution of *rac*-**3a**. The two lines represent formation of (*S*)−(+)-naproxen **4a**. The lower line represents percent conversion up to the maximum (50%). The top line is percent ee. Conditions: *rac*-**3a**, 600 μM, 12C8 (0.5 μM), pH 8.0 (100 mM bicine), 4% DMF, 1% Tween-80, 22 °C.

catalysts with wide potential in biochemistry and organic synthesis.[35] This paper presents the first direct comparison of reactive immunization and transition state analogue hapten manifolds for the elicitation of antibody catalysts. It has revealed that the antibodies that can be generated by each strategy, even for the same reaction, exhibit quite different catalytic behavior. This study has shown that the transition state analogue approach has furnished better biocatalysts in terms of turnover numbers and enantiomeric discrimination, but which possess varying degrees of product inhibition by the phenol **9**. Thermodynamic evaluation reveals that their catalytic power is derived almost entirely as a function of differential stabilization of the transition state over the ground state. In comparison, reactive immunization has elicited biocatalysts which are ultimately more proficient because they couple an efficient "catalytic" mechanism and improved substrate recognition and furthermore do not suffer from product inhibition. Of course this primary study compares only ten antibodies, albeit the five most active from each strategy. Whether the benefits and limitations of each hapten strategy highlighted in this study will prove to be general can only be revealed by further experimentation and comparison in this and other reaction classes.

Experimental Section

General Procedures (Synthesis). As described previously.[11]

Phosphonic Acid Hapten 6. Phosphonate diester **5** (16 mg, 0.02 mmol) was dissolved in THF (2 mL), to which was added LiOH(aq) (0.2 mL, 0.1 M). The reaction mixture was stirred at room temperature for 2 h, then neutralized to pH 3 with 1 N HCl and partitioned with ether. The organic layer was collected and washed with brine, dried ($MgSO_4$), and evaporated to dryness to give the title compound **6** as a white solid (14 mg, 98%): mp 207 °C; ^{1}H NMR (400 MHz, $CDCl_3$) δ 7.90 (d, 2H, J = 7.5 Hz, Ar−H), 7.67 (m, 3H, Ar−H), 7.36 (d, J 7.5 Hz, 1H, Ar−H), 7.05 (m, 2H, Ar−H), 6.90 (dd, J^2_{HP} = 7.8 Hz, Ar−H), 4.25 (t, J 5.6 Hz, 2H, CH_2), 3.81 (dq, 1H, J^2_{HP} = 14.5 Hz, J = 7.5 Hz, CHP), 3.01 (s, 3H, SO_2CH_3), 2.91 (s, 3H, SO_2CH_3), 2.45 (t, J = 6.9 Hz, 2H, CH_2), 1.83 (m, 4H, CH_2), 1.75 (dd, J^2_{HP} = 19.0 Hz, J = 7.3 Hz, 3H, CH_3); ^{13}C NMR (125 MHz, $CDCl_3$) δ 173.37, 166.11, 162.39, 157.11, 136.12, 133.84, 133.81, 132.93, 132.87, 132.75, 129.24, 128.97 (d, J^2_{CP} = 3.6 Hz), 128.58, 128.56, 128.21, 127.23, 127.18, 127.08, 126.96, 119.22, 105.55, 66.35, 44.58, 44.31, 43.71 (d, J^1_{CP} = 27 Hz), 33.91, 28.69, 21.75, 17.75 (d, J^2_{CP} = 6.5 Hz); ^{31}P NMR (101 MHz, $CDCl_3$) δ 23,38; HRFABMS calcd for $C_{25}H_{29}O_8PS$ $(M)^+$ 520.1321, obsd 520.1323.

Antibody Production and Purification. As described previously.[11]

Kinetics. (a) Screening for Catalytic Antibodies. The screening assays were performed in a Bicine (100 mM, pH 8.0) 1% Tween 80 buffer system with 4% DMF as cosolvent. The reaction was followed by monitoring formation of enantiomeric naproxen acids *S*-(+)-4a and *R*-(−)-4b by reversed phase HPLC at 254 nm using a C-18 VYDAC 201TP54 column with an isocratic mobile phase [57% water (0.1% TFA), 43% acetonitrile at 1 mL min^{-1}]. The reaction was initiated by addition of the substrate *rac*-3a, as a solution in DMF (7.5 mM, 20 μL) into a buffer solution with or without antibody (0 μM ≤ [Ab] ≤ 20 μM; 480 μL). At time periods throughout the assay, an aliquot of the reaction mixture was removed (30 μL) and quenched into a solution of the external standard (4-methyl-3-nitroanisole) in water (0.1% TFA)/acetonitrile (1:1; 30 μL). The product concentrations were determined by comparison with product standards.

(b) Kinetic Parameters. The buffer system and HPLC assay were the same as described *vide supra*. To determine the kinetic parameters, the individual enantiomers either *S*-(+)-**3b** or *R*-(−)-**3c** were used as substrates over a range of concentrations up to at least 3 × K_m where possible (1−900 μM) in DMF with an antibody concentration of 0.01−1.5 μM in the aqueous buffer system. The reaction was followed for no more than 5% of the reaction, and as described *vide supra* for only 1−2% of the reaction for the transition state analogue antibodies at high substrate concentrations, during which time the progress curves were linear. Kinetic parameters were calculated using a combination of nonlinear regression and Lineweaver−Burke analyses of the raw data with the EnzymeKinetics v1.1 computer program, Trinity Software (copyright 1990−1991).

(c) Inhibition Constant, K_i Determinations. The K_i values of inhibitors **7** and **8** and phenol **9** (6G6) were determined from their ability to inhibit the hydrolysis of *S*-(+)-**3b** by each member of the reactive immunization and transition state analogue antibody libraries. Because of the problems associated with measuring tight-binding inhibitors where [I] ≈ [Ab], the assays were performed so as to measure the inhibitor concentration required to reduce the enzyme activity to half its original value (IC_{50}) over a broad range of inhibitor concentrations.[25] The antibodies (at concentrations suitable to give good linear rate data) were preincubated with the inhibitor **8** ([6G6] = 30 nM; 1−100 nM **8** and 1−200 μM **9**, [9B1] = 100 nM; 10−1,000 nM **8**, [12C8] = 40 nM; 1−100 nM **8**, [12D9] = 40 nM; 1−100 nM **8**, [11C10] = 500 nM; 100−5000 nM **8**) for 20 min at room temperature. The assay was started by addition of the substrate *S*-(+)-**3b** (either 1.1 × K_m, where possible, or 800 μM) and followed by the HPLC assay described *vide supra*. The K_i was then determined from the IC_{50} by incorporation into eq 1.[25]

(d) Product Inhibition Determination. The effect of phenol **9** (50 μM) and carboxylate **4a** (50 mM) on the catalytic rate of the reactive immunization and transition state analogue antibodies were studied at one concentration of *S*-(+)-**3b** (200 μM). In a typical assay the antibodies (0.01−1.5 μM) in the aqueous buffer solution vide supra (480 μL) were preincubated with either the phenol **9** or acid *S*-(+)-**4a** (2.5 mM in DMF; 10 μL) for 15 min at room temperature. The reaction was initiated by addition of *S*-(+)-**3b** (10 mM in DMF; 10 μL). The rates were measured as described above.

(e) Equilibrium Binding Constant, $K_d$app Determinations. Binding constants were measured in a competition enzyme-linked immunosorbent assay.[36] Polystyrene 96-well plates (Costar) were coated overnight at 4 °C, with a solution of the BSA-5 or BSA-6 conjugate (25 μL of 5 μg mL^{-1}) in PBS (50 mM, pH 7.4). The plates were then blocked with Blotto [4% dry nonfat milk in PBS (50 mM, pH 7.4); 50

(35) Janda, K. D.; Benkovic, S. J.; McLeod, D. A.; Schloeder, D. M.; Lerner, R. A. *Tetrahedron* **1991**, *47*, 2503−2506.

(36) Harlow, E.; Lane, D. P. *Antibodies. A Laboratory Manual*; Cold Spring Harbor Laboratory: Cold Spring Harbor, NY, 1988.

μL per well] at 37 °C and washed with PBS. Stock antibody solutions (50 and 1 μg mL^{-1}) in Bicine (100 mM, pH 8.0, 1%-Tween-8) were diluted to their working concentrations immediately prior to use. After preincubation with stock solutions of inhibitors **7** and **8** (0.1−100 μM; 4 μL in DMF) for 20 min at 37 °C, the antibodies were added to the blocked plates (25 μL per well) and incubated for 1 h at 37 °C. The plate was washed exhaustively with distilled water and a secondary antibody [horseradish peroxidase (HRP)-conjugated goat anti-mouse IgG (1:1500 dilution in Blotto)] (25 μL per well) was applied. The plate was then incubated for 30 min at 37 °C. Following a detergent wash (0.1% Tween-20 in PBS) to remove all nonspecific binders, the plate was developed by addition of tetramethylbenzidine (30 μL). After 20 min, the reaction was quenched by addition of a 2 M solution of H_2SO_4 (30 μL per well) and the absorbance was measured on a Molecular Devices 96-well plate reader at 450 nm.

(f) Enantioselectivity Determination. In a typical assay the antibody (0.5 μM) in the aqueous buffer system described above was incubated with *rac*-**3a** substrate (600 μM). At appropriate time points an aliquot (30 μL) of the reaction mixture was removed and injected directly onto the HPLC. The enantiomers of naproxen acid *S*-(+)-**4a** and *R*-(−)-**4b** were resolved on a Phenomenex chiral HPLC column with an isocratic ammonium acetate (30 mM, pH 4.5) in methanol mobile phase at a flow rate of 2.5 mL min^{-1}; *S*-(+)-**4a** R_T 8.97 min, *R*-(−)-**4b** R_T 12.43 min. The product concentrations were determined by comparisons to product standards and the ee was determined by ratio of peak areas. The reaction was followed until complete conversion of the *S*-(+)-**3b** had been achieved, i.e. 50% conversion.

Acknowledgment. This work was supported by the NIH (GM-43858) and The Skaggs Institute for Chemical Biology.

JA991274T